SEMPA Imaging for Spintronics Applications

J. Unguris, S-H. Chung and D. T. Pierce

National Institute of Standards and Technology, Gaithersburg, MD 20899-8412

Abstract. Scanning Electron Microscopy with Polarization Analysis (SEMPA) provides high resolution (10 nm) magnetization images simultaneously with, but independent of, the topography. Such information is very useful in studying spintronics devices as illustrated by three examples: 1) exchange coupling of magnetic layers, 2) spin-transfer switching in magnetic nanowires, and 3) the ferromagnetic metal-semiconductor interface.

Keywords: nanomagnetism, spintronics, spin polarization, exchange coupling, spin torque transfer, spin reorientation
PACS: 75.70.-i, 75.60.Ch, 75.75.+a, 75.30.Kz

INTRODUCTION

Spintronics, or spin electronics, exploits the spin degree of freedom of the electron in electronic devices resulting in potential advantages such as non-volatility, increased processing speed, and lower power consumption[1]. The discovery of giant magnetic resistance (GMR) provided a tremendous impetus to this field of spin-based electronics[2,3]. GMR was found in structures consisting of thin ferromagnetic layers separated by a layer of non-magnetic material. When the magnetization of each ferromagnetic layer is in the same direction, the resistance of the structure both perpendicular to the layers and parallel to the layers is typically less than when the ferromagnetic layers are antiparallel to each other. A related device is the spin valve in which one ferromagnetic layer is pinned and a second "free" layer, separated from the pinned layer by a non-magnetic layer, can be easily switched in a magnetic field. When the non-magnetic layer is a thin insulator, the electrons tunnel from one ferromagnetic layer to the other in what is called a magnetic tunnel junction (MTJ). Applications for GMR and MTJ devices include magnetic field sensors, read heads for hard drives, and magnetic random access memory (MRAM). These devices, which use ferromagnetic metals, non-ferromagnetic metals and insulators, are sometimes also referred to as magnetoelectronics. There are also emerging device concepts based, for example, on ferromagnetic semiconductors, but to date room temperature operation has not been demonstrated. Taken broadly, spintronics includes both the new emerging devices and the established magnetoelelectronic devices.

A typical spintronic device might contain magnetic layers that are a couple of nanometers thick with a lateral extent of order 100 nm. The control of the magnetization in one or more magnetic layers is crucial to the operation of the device. To characterize such a nanomagnetic device, one would like to be able to observe the magnetization and how it changes. For example, is the magnetization uniform in a single direction, that is, single domain, or are there several domains separated by domain walls? Is the direction of the magnetization in the plane of the magnetic layer or perpendicular to it? How is the magnetization affected by the shape of the nanomagnetic element or by structural defects in it?

We describe in this paper the characterization technique known as scanning electron microscopy with polarization analysis (SEMPA), which in addition to providing the usual SEM topographic image also provides a direct image of the magnetization with high spatial resolution[4,5]. After discussing how SEMPA works, we will illustrate its use with three examples related to spintronics. First, we show a SEMPA measurement of exchange coupled magnetic layers. In this case, spin information is transmitted between the layers without charge movement. In the second example, SEMPA is used to observe how current-induced spin torque can move a domain wall in a ferromagnetic nanowire. This spin transfer process offers new possibilities for changing magnetic states in spintronics devices. The third example examines how the magnetization develops as a ferromagnetic thin film grows on a semiconductor. The ferromagnetic metal-semiconductor heterojunction is important because ferrromagnetic electrodes can be used to inject polarized electrons into a semiconductor.

Semiconductor based spintronic devices will be most easily integrated into existing semiconductor technology.

THE SEMPA TECHNIQUE

The magnetic contrast in scanning electron microscopy with polarization analysis (SEMPA) is due to the fact that secondary electrons emitted from ferromagnets have their magnetic moments parallel, and hence their spins antiparallel, to the magnetization at their point of origin in the sample. As the incident SEM beam is rastered on the sample surface, a measurement of the secondary electron intensity gives the conventional SEM topography image, and a measurement of the secondary electron spin polarization gives a magnetization image[4,5].

The essential parts of the measurement are illustrated schematically in Fig. 1. A typical spin

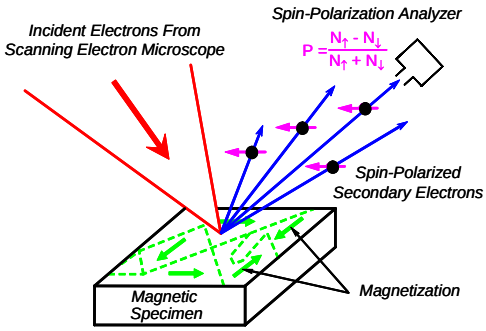

Figure 1. The principle of SEMPA.

analyzer can measure the two components of the spin polarization vector that are transverse to the direction of the detected electron momentum; for example

$$P_x = (N_\uparrow - N_\downarrow)/(N_\uparrow + N_\downarrow), \qquad (1)$$

where $N_\uparrow\,(N_\downarrow)$ is the number of electrons with spins parallel (antiparallel) to the x-direction and $-1 \le P \le 1$. The third component of the polarization, which in our apparatus is the component out of the plane of the sample, can be measured by bending the electron beam 90° into a second detector, so that the out-of-plane component is now transverse to the electron beam. Thus, SEMPA can provide an image of the in-plane and out-of-plane components of the magnetization. Further, as seen from Eq. (1), the polarization is independent of the total intensity, $N_\uparrow + N_\downarrow$, so that the magnetization image is independent of the topography.

An example of a SEMPA measurement of a Fe crystal is shown in Figure 2. The intensity I and two components of the magnetization, in this case M_x and M_y are measured simultaneously. Note that the topography visible in Fig. 2 (c) does not disturb the M_x and M_y images. We frequently find it useful to

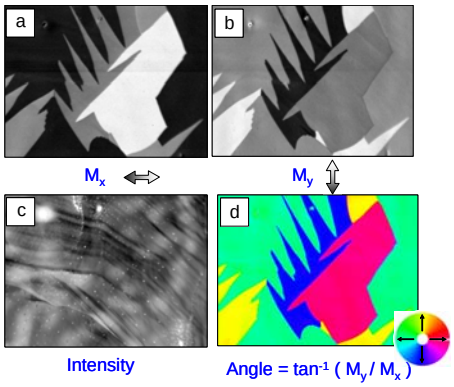

Figure 2. The in-plane horizontal (a) and vertical (b) magnetizations of Fe(100) are measured simultaneously with the topography (c). The direction of the magnetization (d) is derived from (a) and (b).

represent the direction of the magnetization $\theta = \tan^{-1}(M_y / M_x)$ by a color map as shown in Fig. 2 (d). The color wheel gives the magnetization direction. While a topography image can be acquired at video rates, the SEMPA magnetization image, owing to the inefficiency of spin analyzers, requires acquisition times from a minute to an hour depending on the resolution, sample polarization, pixel density, and signal to noise ratio required. At one's disposal are still all the features of the SEM, in particular the magnification and position control to find regions of interest.

Since the magnetic contrast is derived from secondary electrons generated near the sample surface, the magnetic contrast is sensitive to surface contamination. For this reason, an ultrahigh vacuum SEM, such as is typically employed for scanning Auger microscopy, is required for SEMPA. Conventional surface science preparation techniques, such as ion sputtering, and characterization techniques, such as Auger spectroscopy, are routinely used. As in conventional SEM, the samples should have sufficient conductivity to avoid charging. Charging problems can frequently be overcome by depositing a few atomic layers of a metal such as Au or Fe on the surface. SEMPA is sensitive to the spin contribution to the magnetization

$$M = -\mu_B (n_\uparrow - n_\downarrow) \qquad (2)$$

where $n_\uparrow\,(n_\downarrow)$ is the number of spins per unit volume that are aligned parallel (antiparallel) to the magnetization and μ_B is the Bohr magneton. Hence if the magnetization is small compared, for example, to Fe, such as is the case in garnet or even in Permalloy, the secondary electron polarization will also be comparatively small. We have found that the

deposition of a few layers of Fe does not appreciably alter the sample magnetic structure and, owing to the surface sensitivity of SEMPA, greatly enhances the contrast.

Some of the emerging materials for spintronics, such as multiferroics which exhibit both ferromagnetisms and ferroelectricity, are by nature insulators and have a low magnetization. Magnetic semiconductors, such as Ga(Mn)As in which the maximum Mn content is only about 5%, also have a low magnetization. Therefore, decorating the surface with a few layers of Fe will likely be necessary in SEMPA investigations of these emerging spintronic materials to enhance magnetic contrast and/or prevent charging.

APPLICATIONS TO SPINTRONICS

Coupling in Magnetic Heterostructures

Giant magnetoresistance was first discovered in Fe/Cr multilayers in which the Cr thickness was such that in the absence of an applied magnetic field the Fe layers were coupled alternately antiparallel to each other[2,3]. When a field was applied to align the Fe layers, a giant change in the electrical resistance of the magnetic heterostructure was observed. Subsequently it was found that whether the Fe layers were coupled parallel or antiparallel to each other depended on the thickness of the Cr spacer layer[6,7]. Cr is an antiferromagnet, but similar effects were found for Fe layers separated by the noble metals Au and Ag, so this oscillatory exchange coupling effect is more general. Eventually an understanding emerged that the coupling of the magnetic layers depends on the spin dependent reflection amplitudes for Fermi surface electrons in the spacer layer reflecting at the interfaces with the magnetic material[8]. This spin information is transmitted between the ferromagnetic layers without any net charge movement.

The theory also predicts that the sign of the coupling, parallel or antiparallel, oscillates with thickness of the spacer layer. The period or wavelength of the oscillations is determined by the critical spanning vectors between parallel parts of the Fermi surface. Since there are two critical spanning vectors for the nearly free electron like Fermi surface of Au in the [100] direction, the theory predicts a superposition of two periods of oscillations in the exchange coupling in the Fe/Au/Fe(100) multilayer. To compare to these predictions, the experimental system must as closely as possible approximate the theoretical ideal. Irregular interfaces and thickness fluctuations in the interlayer will mask observation of the oscillatory coupling.

We grew nearly ideal Fe/Au/Fe(001) trilayers *in situ* in the SEMPA apparatus[9]. The Au(100) lattice is matched to within 1% of Fe(100) when rotated 45°. While there is a good lattice match in-plane, there is a large out-of-plane mismatch which would lead to growth defects through the Au layer at steps in the surface of the Fe substrate. However, the substrate is an Fe(100) whisker that, after sputtering and annealing in vacuum, has a very flat surface with several hundred nanometers between steps and thus promotes very good growth of the Au interlayer. The deposition is varied to deposit an Au wedge, the thickness of which varies continuously, typically from 0-10 nm over about 1 mm. This is an extremely shallow wedge which is shown schematically and out of proportion in the lower part of Fig. 3. The quality of the growth and the thickness of the Au are monitored using RHEED[10]. Spatially resolved RHEED imaging after the growth of

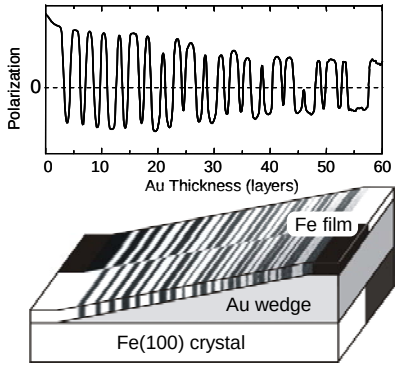

Figure 3. Schematic of the Fe/Au wedge/Fe(100) trilayer with the SEMPA magnetization image overlaid on the top layer. The striking oscillations of the magnetization are seen in the polarization line scan.

the Au wedge permits interlayer thickness measurements to an accuracy of ±0.1 ML. Finally, for the sample in Fig. 3, we deposited a uniform 5 ML thick top layer of Fe.

The SEMPA image of the top Fe layer in Fig. 3 shows the component of magnetization along the whisker. White (black) indicates that M_x is directed in the $+x(-x)$ direction. There are two oppositely oriented domains along the M_x direction in the Fe whisker substrate. In stark contrast, the magnetization of the top Fe layer changes direction many times with varying Au thickness. A total of 43 changes in sign of the coupling are seen in Fig. 3, which together with the precise measurement of the Au thickness allows a precise determination of the two periods of the oscillatory coupling. The coupling periods determined from the SEMPA measurements, 2.48 ML ± 0.05 ML and 8.6 ML ± 0.3 ML, are in agreement with those predicted for the system based on the critical spanning

vectors of the experimental Fermi surface by Bruno and Chappert[11], 2.51 ML and 8.6 ML, thereby providing a very stringent test of the theory.

Spin-Transfer Switching in Nanowires

Current driven domain wall motion offers the exciting prospect of manipulating magnetization in magnetic nanostructures and devices without applying an external magnetic field[12]. As the spin-polarized electrons of an electron current in a ferromagnet pass through a domain wall, there is a torque on the electrons tending to align their spin magnetic moments with the magnetization direction. Conservation of angular momentum requires a reaction torque, known as the spin transfer torque, from the electrons to the magnetization that displaces the domain wall in the direction of electron flow[13]. Here we display high resolution (10 nm) SEMPA magnetization images of transverse and vortex walls in magnetic nanowires and demonstrate the domain wall motion when the current density is sufficiently high[14].

The devices studied consisted of $Ni_{80}Fe_{20}$ nanowires, patterned by electron beam lithography, with widths from 100 nm to 1 μm and thickness from 12 nm to 24 nm. The top of Fig. 4 shows a schematic of such a device including the Al contact pads.

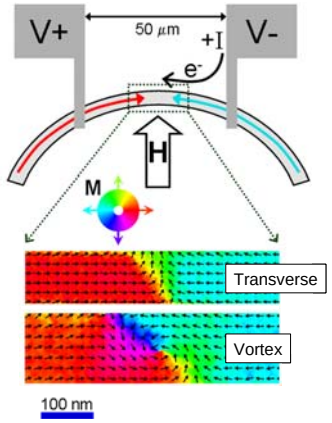

Figure 4. Device schematic showing curved NiFe nanowire. Below, SEMPA images of transverse and vortex domain walls.

When a magnetic field of 80 kA/m (1000 Oe) is momentarily applied perpendicular to the arc, head-to-head or tail-to-tail walls are nucleated in the middle of the arc. The type of domain wall depends on the width and thickness of the nanowire. Two examples are shown at the bottom of Fig. 1: a transverse wall in a 100 nm by 12 nm wire and a vortex wall in a 135 nm by 24 nm wire. While wide wires have vortex walls, very narrow wires can only contain transverse walls which are effectively half of a vortex wall. At some widths and thicknesses, for example a 300 nm by 12 nm wire, we found that applying a current could transform a vortex wall to a transverse wall by pushing the vortex to the edge of the wire; conversely, a vortex could be nucleated at the intersection of a transverse wall with the edge of the wire and move into the wire changing a transverse wall to a vortex wall.

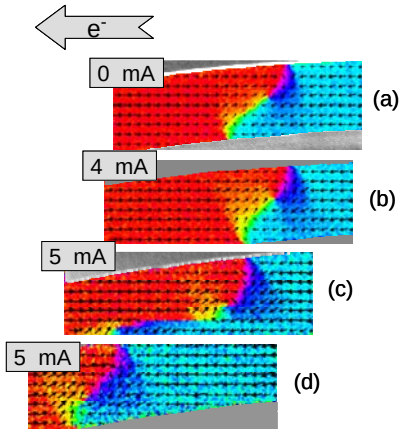

Figure 5. SEMPA images showing the current induced displacement of a vortex domain wall .

SEMPA images showing current induced domain wall motion are shown in Fig. 5. In the top two panels, (a) and (b), the vortex wall is "pinned" and there is no change on increasing the current from 0 to 4 mA. Not much is know about the pinning sites, but it is thought that pinning can be caused by structural defects or chemical inhomogeneities. Nothing is visible in the associated topography image (not shown). Finally in Fig. 5 (c) when 5 mA is applied, the wall is seen to have moved to the left in the direction of electron flow and the vortex has moved down, perpendicular to the flow. The wall jumps about 80% of the way through the image which is scanned from top to bottom. In the image (d) taken immediately after (c), the vortex wall is seen to have moved to the left to be stopped at the next pinning site. If the extrinsic defects that cause pinning can be eliminated or controlled such that they can be tailored to do a particular job, current induced domain wall motion could be used to control the magnetization in spintronic devices.

Ferromagnet-Semiconductor Interface

Many proposed spintronic devices rely on the electrical spin injection from a conventional ferromagnetic metal into a semiconductor. Thin magnetic films can be grown by molecular beam epitaxy (MBE) with crystal structures not found in bulk materials. For example, Co is hcp in the bulk phase at room temperature, but when grown epitaxially on GaAs(110) a bcc structure is stable[15]. Because its majority spin band is nearly completely

filled, bcc Co is particularly attractive as an electrode for spintronic devices.

SEMPA was used to investigate the details of the thickness dependence of the variations in the magnetic properties of Co/GaAs(110)[16]. Co was deposited by electron beam evaporation onto GaAs(110) at room temperature. A shutter scanned in front of the

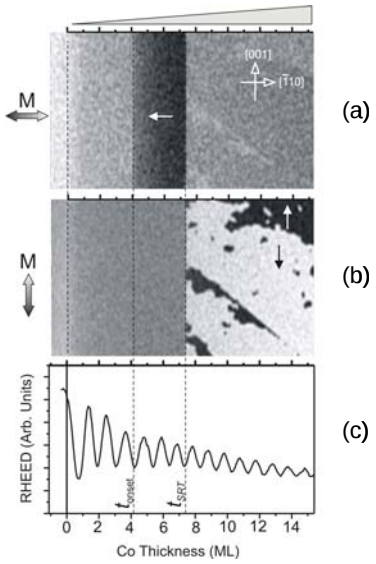

Figure 6. The x component (a) and y component (b) of a 124 x 74 μm magnetization image of a Co wedge on GaAs(110). (c) RHEED intensity oscillations measured along the wedge.

substrate created a Co wedge varying in thickness from 0 up to 30 ML. The two in-plane components of the magnetization are imaged from the first part of such a wedge in Fig. 6 (a) and (b). The thickness of the Co film at each point along the wedge was precisely determined by spatially resolved RHEED intensity oscillations measured in the SEM and shown in Fig. 6 (c).

MBE Co films grown on GaAs(110) exhibit three distinct magnetic regions. For Co films up to about 4 ML, no magnetization is observed as is evident in Fig. 6. This magnetically dead phase explains the origin of the reduced magnetic moment observed by others at the Co/GaAs interface. The scanning Auger spectroscopy capability of our SEM provides a map of the chemical composition along the wedge. The formation of an interfacial Co_2GaAs alloy is observed up to about 3.4 ML. The onset of ferromagnetism at room temperature measured by SEMPA is thought to correspond to the coalescence of Co islands that grow on this alloy phase. As seen from Fig 6, the film is initially magnetized along the x axis. However, at a thickness of 7.1- 7.4 ML ±0.3ML, depending on sample, there is an abrupt in-plane spin reorientation transition of the easy axis from $[\bar{1}10]$ to [001]. Above the spin reorientation transition the domain structure is strikingly different with many irregularly shaped head-to-head domain walls. This change in the direction of the easy axis can be understood in terms of the competition between surface and bulk magnetic anisotropies. Clearly such details of the interface between ferromagnetic metals and semiconductors have to be understood and controlled in order to optimize spintronic devices.

ACKNOWLEDGMENTS

This work was supported in part by the Office of Naval Research.

REFERENCES

1. S. A. Wolf et al., Science **294**, 1488 (2001).
2. M. Baibich et al., Phys. Rev. Lett. **61**, 2472 (1988).
3. J. Barnas et al., Phys. Rev. B **42**, 8110 (1990).
4. M. R. Scheinfein et al., Rev. Sci. Instrim. **61**, 2501 (1990).
5. J. Unguris, "SEMPA and its Applications," in *Experimental Methods in the Physical Sciences* **36**, edited by M. De Graef and Y. Zhu, Academic Press, New York (2001) p. 167-194.
6. S.S.P. Parkin, N. More, and K. P. Roche, Phys Rev. Lett. **64**, 2304 (1990).
7. J. Unguris, R. J. Celotta, and D. T. Pierce, Phys. Rev. Lett. **67**, 140 (1991).
8. M. D. Stiles, Phys. Rev. B **48**, 7238 (1993).
9. J. Unguris, R. J. Celotta, and D. T. Pierce, J. Appl. Phys. **75**, 6437 (1994).
10. D. T. Pierce, J. Unguris, and R. J. Celotta, "Investigation of Exchange Coupled Layers with SEMPA," in *Ultrathin Magnetic Structures* edited by B. Heinrich and J.A.C. Bland, Springer-Verlag, New York (1994) p. 117-147.
11. P. Bruno and C. Chappert, Phys. Rev. Lett. **67**, 1602 (1991).
12. L. Berger, J. Appl. Phys. **49**, 2156 (1978); **55**, 1954 (1984).
13. M. D. Stiles and A. Zangwill, Phys. Rev. B **66**, 014407 (2002).
14. W. Casey Uhlig and J. Unguris (to be published)
15. G. A. Prinz, Phys. Rev. Lett. **54**, 1051 (1985).
16. T. L. Monchesky and J. Unguris, Phys. Rev. B. **74**, 241301(R) (2006).